Bioconjugate Chemistry

ARTICLE

pubs.acs.org/bc

Efficient Orthogonal Bioconjugation of Dendrimers for Synthesis of Bioactive Nanoparticles

Hubert F. Gaertner,[†] Fabrice Cerini,[†] Arun Kamath,[‡] Anne-Françoise Rochat,[‡] Claire-Anne Siegrist,[‡] Laure Menin,[§] and Oliver Hartley*[,†]

[†]Department of Structural Biology and Bioinformatics, Faculty of Medicine

[‡]Departments of Pathology-Immunology and Pediatrics, University of Geneva, 1 Rue Michel Servet, 1211 Geneva 4, Switzerland

[§]Service de Spectrométrie de Masse de l'ISIC (SSMI), EPFL, Bât. Chimie (BCH 1524), CH-1015 Lausanne, Switzerland

Supporting Information

ABSTRACT: Nanoparticles carrying biologically active functional sets (e.g., targeting moiety, payload, tracer) have potential use in a wide range of clinical applications. Though complex, such constructions should, as far as possible, have a defined molecular architecture and be monodisperse. However, the existing methods to achieve this goal are unsuitable for the incorporation of peptides and proteins, and those that provide for orthogonal introduction of two different types of functional element are incompatible with the use of commercially available materials. In this study, we have developed approaches for the production of nanoparticles based on commercially available polyamidoamine (PAMAM) dendrimers. First, we identified an optimized oxime conjugation strategy under which complex dendrimers can be fully decorated not only with model peptides, but also with recombinant proteins (insulin was taken as an example). Second, we developed a strategy based on a two-chain covalent heterodendrimer (a "diblock") based on cystamine core PAMAM dendrimers and used it to generate heterodendrimers, into which a peptide array and a mannose array were orthogonally introduced. Finally, by incorporating a functionalized linker into the diblock architecture we were able to site-specifically introduce a third functional element into the nanoparticle. We exemplified this approach using fluorescein, a mannose array, and a peptide array as the three functionalities. We showed that incorporation of a mannose array into a nanoparticle strongly and specifically enhances uptake by sentinel cells of the immune system, an important property for vaccine delivery applications. These PAMAM dendrimer-based approaches represent a robust and versatile platform for the development of bioactive nanoparticles.

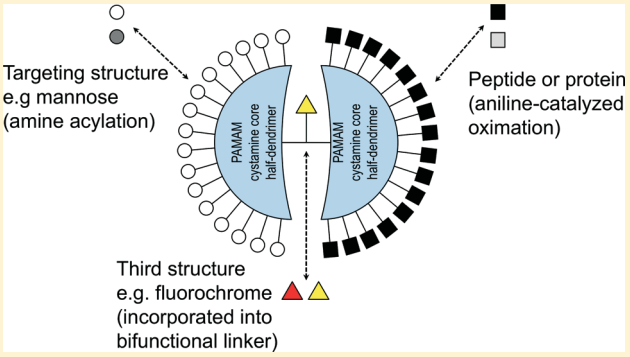

INTRODUCTION

Dendrimers are branched polymers synthesized in a stepwise manner from a central core to generate particles that combine a precise, potentially monodisperse molecular architecture carrying a high density of surface functional groups. These properties make dendrimers attractive scaffolds for the generation of bioactive nanoparticles for clinical applications including drug and gene delivery, tumor targeting, bioimaging, tissue remodelling, generation of antiviral products, and vaccine delivery.[1−3]

For these uses, it is highly desirable to obtain fully decorated scaffolds, thereby maximizing the possible benefits to biological activity of multivalent display,[4] as well as ensuring homogeneity and reproducibility from batch to batch and within each batch. While close to complete decoration of large, complex dendrimers has been achieved in the development of sugar arrays,[5,6] decoration with peptides and proteins has proven to be more challenging. None of the peptide/protein conjugation chemistry approaches explored so far, including hydrazone and oxime chemistry,[7,8] native chemical ligation,[9] click chemistry,[10,11] and noncovalent synthesis of protein dendrimers,[12] have proven powerful enough to fully decorate dendrimers more complex than tetramers and octamers.

A second challenge lies in developing the capacity to orthogonally introduce more than one active substituent into the nanoparticle architecture (e.g., a targeting moiety, a drug payload, a fluorescent tracer).[1,2] Approaches that enable multiple functional units to be independently attached to dendrimers via precision conjugation would be of significant value, enabling the copy numbers of different functional units to be optimized independently of one another. While several different strategies for the production of heterodendrimers carrying two different functional units have been presented,[8,13,14] none of these are

Received: December 13, 2010
Revised: May 13, 2011
Published: May 16, 2011

dx.doi.org/10.1021/bc1005653 | *Bioconjugate Chem.* 2011, 22, 1103–1114

Scheme 1. Diblock Approach Based on Cystamine Core PAMAM Dendrimers for the Preparation of Heterodendrimers Carrying Protein/Peptide Plus an Additional Functional Unit Set

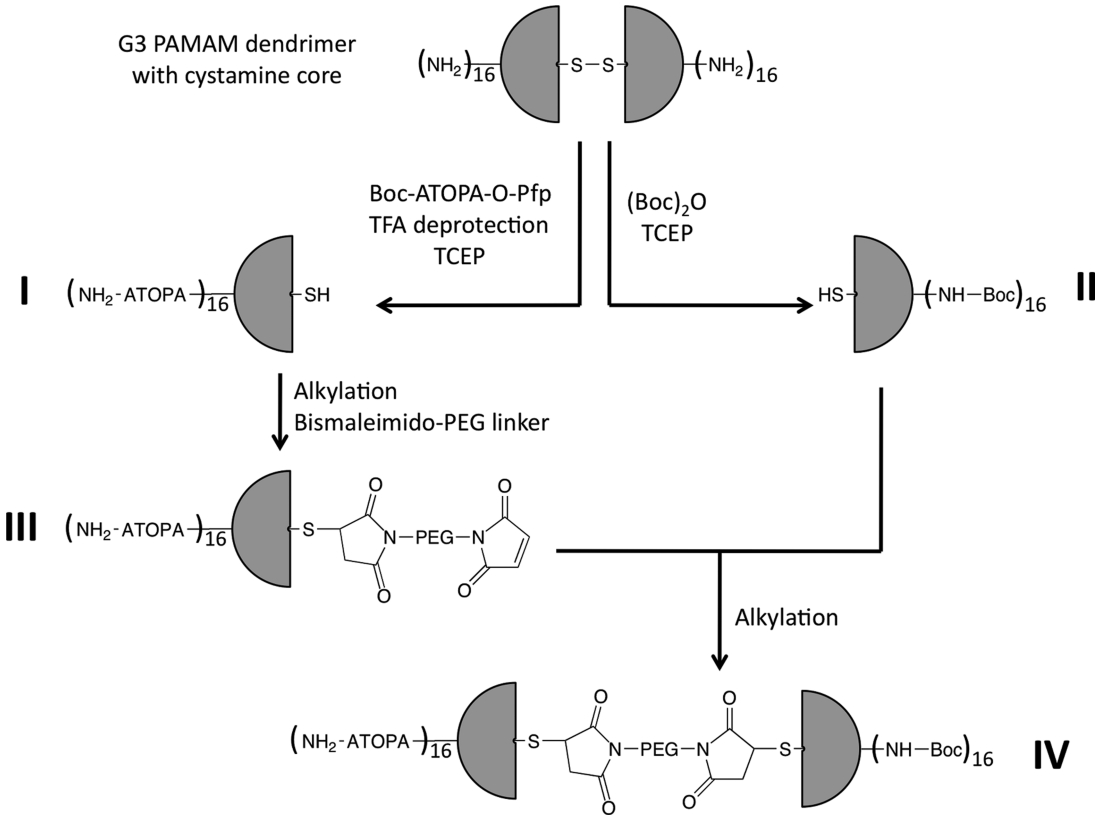

compatible with the use of commercially available dendrimers as starting materials.

In this study, we present a robust strategy for conjugation of commercially available polyamidoamine (PAMAM) dendrimer scaffolds with peptides and proteins. This work is based on oxime chemistry, building on two recent discoveries in the field: first, that an alkoxyamine reacts much more readily with pyruvic acid than with N-terminal glyoxyl groups,[15] and second, that oxime ligation can be significantly accelerated and provide quantitative yields when aniline is used as a small-molecule organocatalyst.[16,17]

We have also developed an orthogonal diblock strategy for the generation of heterodendrimers from PAMAM dendrimers carrying a cystamine core. This approach is centered on the production of a key intermediate structure (Scheme 1) that is subsequently (i) acylated on the surface amines of one-half-dendrimer, those of the other half-dendrimer being temporarily protected and, following deprotection of the latter, (ii) decorated with an array of oxime-conjugated peptides on the other (Scheme 2). We exemplified this approach by producing G-3 heterodendrimers in which one half-dendrimer is decorated with mannose and the other with peptide.

A potentially useful application of mannose−peptide/protein nanoparticles is in vaccine delivery: directly targeting a peptide or protein antigen to mannose-receptor-expressing sentinel cells of the immune system by incorporating it into a mannose-coated particle.[18−21] We produced such a heterodendrimer, further enhanced by the functionalization of the linkage between the two halves with fluorescein. This fluorescent mannose−peptide heterodendrimer was used to demonstrate the effect of incorporating a mannose array on the specific uptake of nanoparticles by dendritic cells and macrophages.

EXPERIMENTAL PROCEDURES

General Methods. Unless stated otherwise, all solvents and other chemicals were obtained from commercial sources and used as received. Amine-terminated PAMAM dendrimers were supplied by Sigma-Aldrich and Dendritic Nanotechnologies (Mount Pleasant, MI, USA). Analytical reverse-phase high-pressure liquid chromatography (HPLC) was performed on a Waters 2795 HPLC module coupled with 214 nm UV detection, using a Macherey Nagel 300A, 5 μm C8 column. Preparative HPLC was performed on a Delta 600 module coupled with a 2487 UV detector using a Vydac C8 column (250 × 22 mm i.d., 10 μm particle size) under previously described conditions.[17] Electrophoresis of peptide and protein constructs was performed on NuPage 12% Bis-Tris Gel from Invitrogen (MOPS buffer, 100 V). Matrix-assisted laser desorption/ionization time-of-flight mass spectrometry (MALDI-TOF-MS) spectra were obtained on a Perspective Biosystems Voyager SSTR or on a Shimadzu AXIMA CFR Plus mass spectrometer using sinapinic acid, 2,5 dihydroxybenzoic acid, or 2′,4′,6′-trihydroxyacetophenonemonohydrate as matrix. Electrospray ionization mass spectrometry (ESI-MS) spectra were measured on either a MicroMass Quattro Micro Mass Spectrometer or a Waters Q-TOF Ultima Mass Spectrometer, both used in positive ionization mode.

Generation of Pyruvate Dendrimers. *Succinimide Activated Pyruvate (pyruvate-OSu).* Pyruvate succinimide ester was prepared by activation of pyruvic acid (50 mg/mL) with 1 equiv dicyclohexylcarbodiimide and 1 equiv N-hydroxysuccinimide in CH_2Cl_2. The mixture was stirred overnight and filtered to remove the dicyclohexylurea precipitate. The solvent was evaporated

Scheme 2. Production of Mannose−Peptide Heterodendrimers

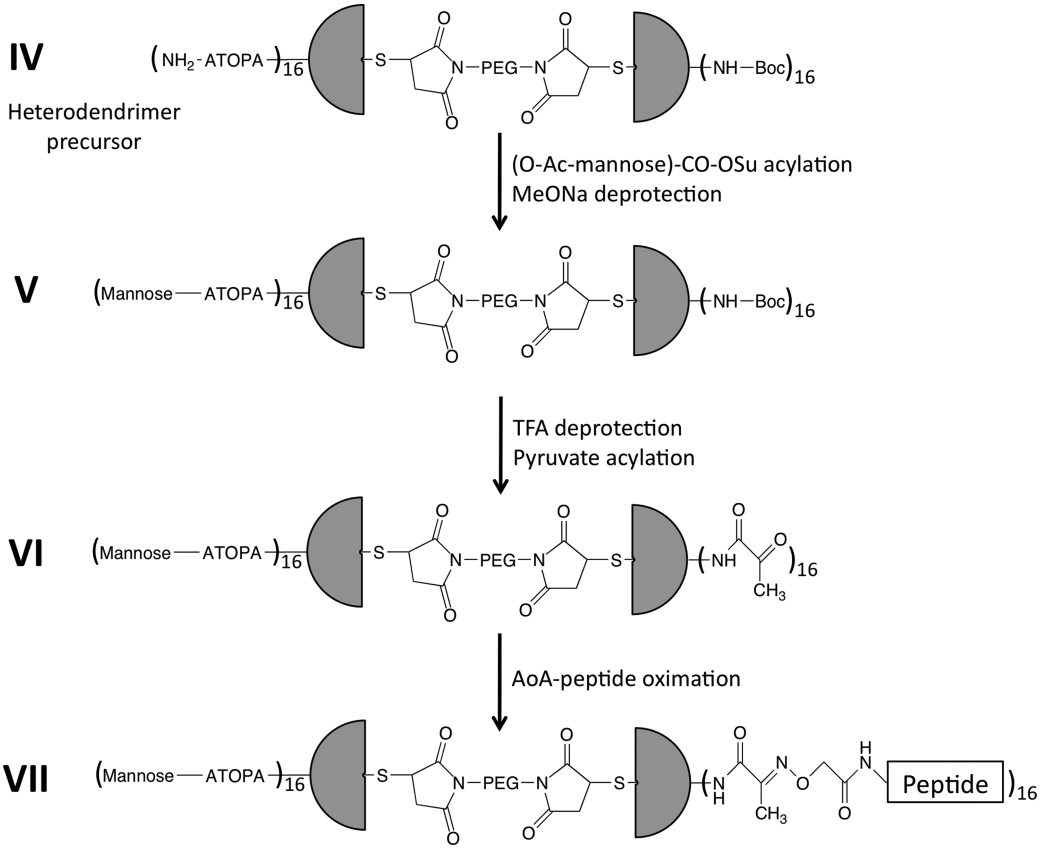

using reduced pressure, and the powder obtained was used without further purification.

PEG-Elongation of Dendrimer Arms. Where required, dendrimer arms were elongated with Boc-amino-PEG-COOH chains (either 2-[2-(Boc-amino)ethoxy]ethoxy}acetic acid (Boc-AEEA) or Boc-15-amino-4,7,10,13-tetraoxapentanedecanoic acid (Boc-ATOPA)), activated by esterification with pentafluorophenol (see Supporting Information for details of synthesis).

Dendrimer Functionalization. The dendrimer solution obtained from the supplier (20% w:v in MeOH) was diluted with 9 vol of CH_2Cl_2 containing 5 equiv of pyruvate-OSu per amino group. The solution was stirred overnight at room temperature and reaction completion was verified by the Kaiser test.[22] The solution was then concentrated under reduced pressure and the material resolubilized in CH_3CN/water (1:1 v/v) containing 0.1% w/v trifluoroacetic acid (TFA). The soluble fraction was further purified by preparative HPLC, using a 0−50% gradient elution system between 0.1% (w/v) TFA (solvent A) and acetonitrile/TFA/water, 900:1:100 (v:w:v) (solvent B) over 50 min, at 15 mL/min.

Conjugation of Pyruvate Dendrimers with Aminooxy-Functionalized Peptides and Insulin. The linear peptides LYRAG (Leu-Tyr-Arg-Ala-Gly) and the measles virus hemeagluttenin-derived peptide MVHA49−72 (Leu-Ile-Gly-Leu-Leu-Ala-Ile-Ala-Gly-Ile-Arg-Leu-His-Arg-Ala-Ala-Ile-Tyr-Thr-Ala-Glu-Ile-His-Lys) were synthesized according to standard automated techniques as previously described.[23] They were substituted at their α-amino groups with the aminoxyacetyl group (AoA), protected with the Boc function by reaction with Boc-aminooxyacetyl-OSu. AoA-Phe^{B1}-insulin was prepared according to standard techniques.[7] The derivatized products were single components on HPLC and had the expected mass spectra when analyzed by ESI-MS.

All conjugation experiments were performed in a 0.1 M acetate buffer containing 20% CH_3CN (v:v) or 8 M urea and 0.1 M anilinium acetate, pH 4.6. AoA-derivatized products (1.5−2.0 equiv) were mixed with 1 equiv of pyruvate dendrimer, and the reaction was allowed to proceed at room temperature for 20−40 h. The conjugation products were isolated by HPLC or, in the case of MVHA (49−72) conjugates, by dialysis.

Construction of Diblock Dendrimer Template. *G-3(ATOPA-NH_2)$_{16}$-S-PEG-maleimide (II in Scheme 1). Extension of Cystamine Core Dendrimer Arms with ATOPA Linker.* Boc-ATOPA-pentafluorophenyl ester (300 mg; for details of synthesis, see Supporting Information) was solubilized in 1 mL CH_2Cl_2 and added to 300 μL of a solution of G-3 cystamine core dendrimer (20% w/v in MeOH) at a 2-fold molar excess with respect to dendrimer surface amino groups. After overnight incubation at 20 °C, reaction completion was verified using a ninhydrin test. The reaction medium was then concentrated, solubilized in MeOH/CH_2Cl_2 (1:1 v/v), and purified on a LH-20 column equilibrated in the same solvent mixture.

Reduction of Cystamine Core to Produce Half-Dendrimers. The purified product (**I** in Scheme 1; 130 mg) was then deprotected in 4 mL TFA for 10 min at room temperature. TFA was removed under vacuum, and the remaining material was taken up in water and freeze−dried. This material was resuspended in 4 mL water, mixed with 1 mL of a 0.1 M tris(2-carboxyethyl)phosphine solution, and the pH adjusted to 5.0 with 1 M NaOH. After 2 h incubation at 20 °C, the material was purified by preparative

dx.doi.org/10.1021/bc1005653 |*Bioconjugate Chem.* 2011, 22, 1103–1114

HPLC on a C8 column using a 0−50% solvent B gradient over 50 min. The isolated material was characterized by ESI-MS (observed average mass 7456.9 ± 0.9 Da; calculated 7458.8 Da).

Attachment of Linker to Half-Dendrimer Sulfhydryl Group. 50 mg of the previous material was alkylated with a 2-fold molar excess of bismaleimido-4,7,10-trioxa-1,13-tridecanediamine linker (for linker synthesis, see Supporting Information) in a 0.1 M MES, 5 mM EDTA buffer pH 6.0 containing 50% CH_3CN. After 2 h incubation at 20 °C, the alkylated material (**III** in Scheme 1) was isolated by preparative HPLC and characterized by ESI-MS (observed average mass 8008.2 ± 0.4 Da; calculated 8008.4 Da). Material recovered: 44 mg.

*G-3(NH-Boc)$_{16}$-SH (**II** in Scheme 1).* A solution (300 μL) of a cystamine core G-3 dendrimer (20% (w:v) in MeOH) was added to $(Boc)_2O$ (5-fold molar excess over dendrimer surface amine groups) dissolved in 1 mL CH_2Cl_2. After overnight incubation at 20 °C, the material was purified on a LH20 column equilibrated in MeOH:CH_2Cl_2, 1:1 (v:v), and dried. The recovered material (65 mg) was solubilized in 3 mL MeOH:water 1:1 (v/v), TCEP was added to final concentration of 20 mM, and the pH was adjusted to 5.0 with 1 M NaOH. After 2 h incubation at 20 °C, the material was purified by preparative HPLC on a C4 column using a 20−60% B gradient over 40 min. Material recovered: 37 mg.

*G-3(ATOPA-NH$_2$)$_{16}$-S-PEG-S-G-3(NH-Boc)$_{16}$ (**IV** in Scheme 1).* Some 30 mg G-3(NH-Boc)$_{16}$-SH (**II** in Scheme 1) was reacted with a 1.5 molar excess of G-3(ATOPA-NH$_2$)$_{16}$-S-PEG-maleimide (**III** in Scheme 1) in 4 mL 50% MeOH containing 0.1 M MES, 5 mM EDTA, pH 6.0. After 3 h incubation at room temperature, the conjugation product (**IV** in Scheme 1) was purified by preparative HPLC on a C4 column and characterized by ESI-MS (observed average mass 13 112.9 ± 0.3 Da; calculated average mass 13108.9Da). Material recovered: 39 mg.

Production of Mannosylated Heterodendrimers. *Coupling Mannose to Unprotected Surface Amines.* Coupling of the succinimide ester of 3-(2,3,4,6-tetra-*O*-acetyl-α-D-mannopyranosylthio) propionic acid (see Supporting Information for details of synthesis) with G-3(ATOPA-NH$_2$)$_{16}$-S-PEG-S-G-3(Boc)$_{16}$ was carried out at 50 mg/mL in a MeOH/CH_2Cl_2 (1:1, v/v) at 20 °C for 15 h using a 2-fold molar excess of the activated ester with respect to the primary amino groups on the dendrimer, with a 3-fold excess of *N*-methylmorpholine. Complete acylation was verified using the ninhydrin test, and the carbohydrate dendrimer was isolated by chromatography on a LH20 column equilibrated in MeOH/CH_2Cl_2 (1:1 v/v). Material recovered: 37 mg. Deprotection of the acetylated mannose−dendrimer was achieved by treating the sample in MeOH/water (1:1 v/v) at 10 mg/mL at room temperature to which catalytic amounts of 0.3 M methanolic solution of MeONa (a total of 1 mol MeONa per mole of sugar 5−6 days) were added so that the pH was maintained at 8.5. The reaction was followed by analytical HPLC and considered to be complete after a total shift of the initial material into a more hydrophilic, symmetrical peak after 5−6 days of incubation.

Boc-Deprotection and Pyruvate Acylation. The resulting material was isolated by preparative HPLC on a C4 column, Boc-deprotected in neat TFA at 10 mg/mL for 5 min at room temperature, dried, and acylated with a 5-fold molar excess of Pyr-OSu under the same conditions used for homodendrimers (see pyruvate acylation) except that *N*-methylmorpholine was added to neutralize dendrimer solution in MeOH. The Boc-deprotected intermediate was characterized by MALDI-TOF-MS: observed envelope of 12 000−16 000 with an apex at 15000; calculated average mass: 15511.6 Da.

Peptide Oximation. Conjugation with AoA-LYRAG (AoA-Leu-Tyr-Arg-Ala-Gly) was carried out as for homodendrimers (see above) in 0.1 M sodium acetate buffer (pH 4.6) containing 20% CH_3CN (v:v) and 0.1 M anilinium acetate, using a 1.5−2.0 molar excess of peptide over dendrimer pyruvate groups. The conjugation product was isolated after 20 h incubation at room temperature by HPLC.

Construction of Fluorescein-Labeled Homo- and Heterodendrimers. *G-3(ATOPA-NH$_2$)$_{16}$-S-FAM.* G-3(ATOPA-NH$_2$)$_{16}$-SH (15 mg, **I** in Scheme 2) was alkylated with a 5-fold excess of 4-iodoacetamidofluorescein (4-iodoacetamido-FAM) in 1 mL of semiaqueous buffer of 50 mM NaH_2PO_4, 5 mM EDTA, containing 50% acetonitrile at pH 7.0. After 2 h incubation at room temperature, the conjugation product was isolated by preparative HPLC and characterized by ESI-MS (observed average mass 7845.6 ± 1.1 Da; calculated average mass 7847.1 Da). Material recovered: 12 mg.

G-3(ATOPA-Mannose)$_{16}$-S-FAM. G-3(ATOPA-NH$_2$)-S-FAM was acylated with a 2-fold molar excess of the succinimide ester of 3-(2,3,4,6-tetra-*O*-acetyl-α-D-mannopyranosylthio) propionic acid as described above. Material was purified after deprotection by gel filtration on a Phenomenex S2000 column equilibrated in 20% CH_3CN containing 0.1% TFA. Material recovered: 10 mg.

G-3(ATOPA-Pyr)$_{16}$-S-FAM. G-3(ATOPA-NH$_2$)-S-FAM (7 mg) was acylated with a 5-fold molar excess of Pyruvate-OSu in the presence of 3 equiv of *N*-methylmorpholine per free amino group in a MeOH/CH_2Cl_2 (1:1) mixture overnight at room temperature. The reaction medium was dried, purified by preparative HPLC, and characterized by ESI-MS (observed average mass 8966.3 ± 0.6 Da; calculated average mass 8968.1 Da. Material recovered: 8 mg.

G-3(ATOPA-Pyr=AoA-LYRAG)$_{16}$-S-FAM. AoA-LYRAG was conjugated to G-3(ATOPA-Pyr)$_{16}$-S-FAM by 48 h reaction at room temperature at a concentration of 0.2 mM using a 2-fold excess of peptide (with respect to the number of pyruvate functional groups on the dendrimer) in a buffer containing AcONa 0.1 M: CH_3CN (4:1 v/v) and 0.1 M anilinium acetate, pH 4.6. The conjugate was isolated by semipreparative HPLC on a C8 column and characterized by MALDI-TOF-MS (observed average mass for the highest substituted entity 19 143 Da (Na adduct); calculated mass 19 108).

G-3(ATOPA-Mannose)$_{16}$-S-AEEA-Lys(FAM)-ADOOA-S-G-3-(Pyruvate)$_{16}$ (bm). Construction of the heterodendrimer via a maleimido-AEEA-Lys(FAM)-ADOOA-maleimide linker (bm, see Supporting Information for details of synthesis) was carried out as with the nonlabeled PEG linker for the synthesis of G-3(ATOPA-NH$_2$)$_{16}$-S-PEG-S-G-3(NH-Boc)$_{16}$ (see above).

G-3(ATOPA-Mannose)$_{16}$-S-AEEA-Lys(FAM)-ADOOA-S-G-3-(Pyruvate)$_{16}$ (iac). The G-3(Boc)$_{16}$-SH half-dendrimer was alkylated with an iodoacetamide-AEEA-Lys(FAM)-ADOOA-iodoacetamide linker (iac, see Supporting Information for details of synthesis) by reacting a 2-fold molar excess of linker with the dendrimer in 0.1 M NaH_2PO_4 buffer containing 5 mM EDTA and 50% CH_3CN, pH 7.0. The conjugate was isolated by preparative HPLC on a C4 column, after overnight incubation, and characterized by ESI-MS (average observed mass 6091 ± 3 Da, calculated mass 6088 Da). The resulting material (2.1 μmol) was then reacted at room temperature with a 1.5-fold molar excess of G-3(ATOPA-NH$_2$)-SH in 0.1 M NaH_2PO_4 buffer containing 5 mM EDTA and 50% MeOH, pH 7.0, and the conjugate was isolated after 24 h incubation and characterized by ESI-MS (average observed mass 13 420.4 ± 2.9 Da, calculated mass 13 419.2 Da).

Table 1. Mass Spectrometric Characterization of Pyruvate-Conjugated Dendrimers

dendrimer	calculated average mass (Da)	observed mass (Da) ESI-MS
G-1$(Pyr)_8$	1990.4	1990.4 ± 0.4
G-2$(Pyr)_{16}$	4377.0	4376.7 ± 0.1[a]
G-3$(Pyr)_{32}$	9150.9	9170.1 ± 0.8[a]
G-1$(AEEA\text{-}Pyr)_8$	3151.8	3151.5 ± 0.1
G-2$(ATOPA\text{-}Pyr)_{16}$	8333.9	8333.4 ± 0.5

[a] ESI-MS spectra also identified contaminating products of 200 Da lower mass than the expected value (spectra are provided in Supporting Information).

Further functionalization with mannose and pyruvate was carried out as described for the nonfluorescent heterodendrimers.

Isolation of Lymph Node Dendritic Cells and Macrophages and Uptake Experiments. Balb/c mice (8−10 weeks old, Charles River Laboratories, L'Arbresle, France) were bred and kept according to requirements of the University of Geneva and Swiss and European guidelines. Single-cell suspensions of inguinal, axial, and brachial lymph nodes were prepared by enzymatic digestion as described.[24]

Cells (2×10^6 in 200 μL) were incubated with dendrimer preparations for 1 h at 37 or 4 °C. Cells were then preincubated with rat anti-CD16/32 mAb (2.4G2 clone) to block nonspecific antibody binding, and stained with conjugated antibodies against CD11c (HL3 clone), CD11b (M1/70 clone), and B220/CD45R (RA3−6B2 clone) (BD Pharmingen, San Diego, CA). Each sample was acquired on a FACS Canto cytometer and data were analyzed using *FlowJo* software (Tree Star, Ashland, OR). Total lymph-node cells were determined by forward/side scatter. Within this gate, $CD11c^+$ cells were taken to be dendritic cells, $CD11b^+$ $CD11c^-$ cells were taken to be macrophages, and $B220^+$ $CD11c^-$ $CD11b^-$ cells were taken to be B lymphocytes.

RESULTS

Pyruvate Conjugation of Dendrimers. Pyruvate dendrimers were successfully synthesized by acylation of the amine terminal groups of G-1, G-2, and G-3 PAMAM dendrimers with succinimide−activated pyruvate to yield G-1$(Pyr)_8$, G-2$(Pyr)_{16}$, and G-3$(Pyr)_{32}$ (see Scheme 1). Pyruvate acylation was also carried out on dendrimers of which the arms had been elongated through acylation with the amino-PEG-acids 2-[2-(Boc-amino) ethoxy]ethoxy}acetic acid (Boc-AEEA) and Boc-15-amino-4,7,-10,13-tetraoxapentanedecanoic acid (Boc-ATOPA) to yield G-1-$(AEEA\text{-}Pyr)_8$ and G-2$(ATOPA\text{-}Pyr)_{16}$.

All pyruvate conjugation reactions went to completion as determined by the ninhydrin test for remaining free amines. The resulting pyruvate dendrimers had the expected masses (Table 1) except the G-2$(Pyr)_{16}$ and G-3$(Pyr)_{32}$ pyruvate dendrimers, which gave ESI-MS data consistent with contaminating products of 200 Da lower mass than the expected value (spectra are provided in Supporting Information). These lower-mass products are most likely derived from lower-valency contaminants in the starting material. A loss of 200 Da corresponds not just to the lack of two pyruvate units but to the absence of two complete −$(NHCH_2CH_2NH\text{-pyruvate})$ units. Such contamination of higher-generation dendrimers with material lacking two terminal amine groups has been described.[6] The phenomenon is thought to be due to the formation of an intramolecular bis-amide instead of the addition of two ethylene diamines during manufacture.

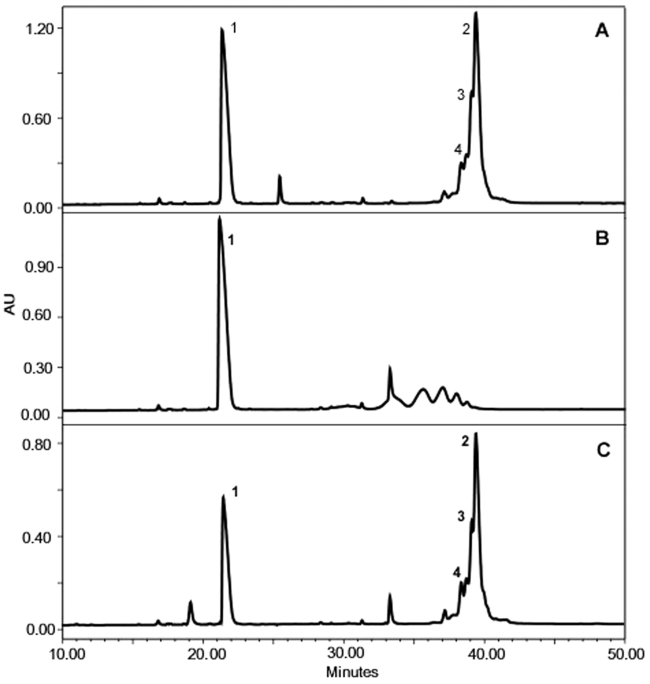

Figure 1. Importance of aniline catalysis for full decoration of pyruvate dendrimers by AoA-peptides and proteins. HPLC analyses of polyoxime formation after 15 h incubation at room temperature at various pH values, monitored at 214 nm. Reactions were carried out on 50 nmol G1-$D(Pyr)_8$ using 1.5 equiv AoA-LYRAG per dendrimer Pyr- group (excess elutes at 21.5 min). Peak 1 corresponds to the excess of AoA-peptide and peak 2 to the target octaoxime, while peaks 3 and 4 correspond to lower valency constructs (hexa- and pentaoxime). Trace A, reaction at pH 3.0 without anilinium acetate; trace B, reaction at pH 4.6; trace C, reaction at pH 4.6 in the presence of 0.1 M anilinium acetate.

Optimizing Conditions for Conjugation of Proteins and Peptides. The conditions for pyruvate−dendrimer conjugation with aminooxy-functionalized peptides and proteins were first optimized using the G-1$(Pyr)_8$ dendrimer and a small model peptide, AoA-LYRAG. Under previously established standard conditions for oxime ligation[7] but using pH values between 2 and 3 instead of the usual value of 4.6, the reaction goes essentially to completion (Figure 1A), with the hexa- and penta-oxime contaminants likely to have resulted from the decoration of lower-valency contaminants in the original dendrimer preparation (see above). Carrying out the reaction at pH 4.6 results in the formation of a mixture of conjugates containing mainly partially substituted intermediates and only traces of the fully substituted octamer (Figure 1B). When the reaction is carried out at pH 4.6 in the presence of 0.1 M aniline, however, the reaction goes essentially to completion (Figure 1C), yielding the fully substituted octamer together with the hexa- and penta-oxime contaminants seen in Figure 1A (these are also likely to have resulted from the decoration of lower valency contaminants in the original dendrimer preparation).

Evaluation of Mass Spectrometric Characterization Methods. Characterization of complex dendrimers with large peptide and protein substituents presents a methodological challenge, and we opted to evaluate ESI-TOF-MS (electrospray ionization time-of-flight mass spectrometry) and MALDI-TOF-MS as characterization tools. As reference materials, we used the octameric

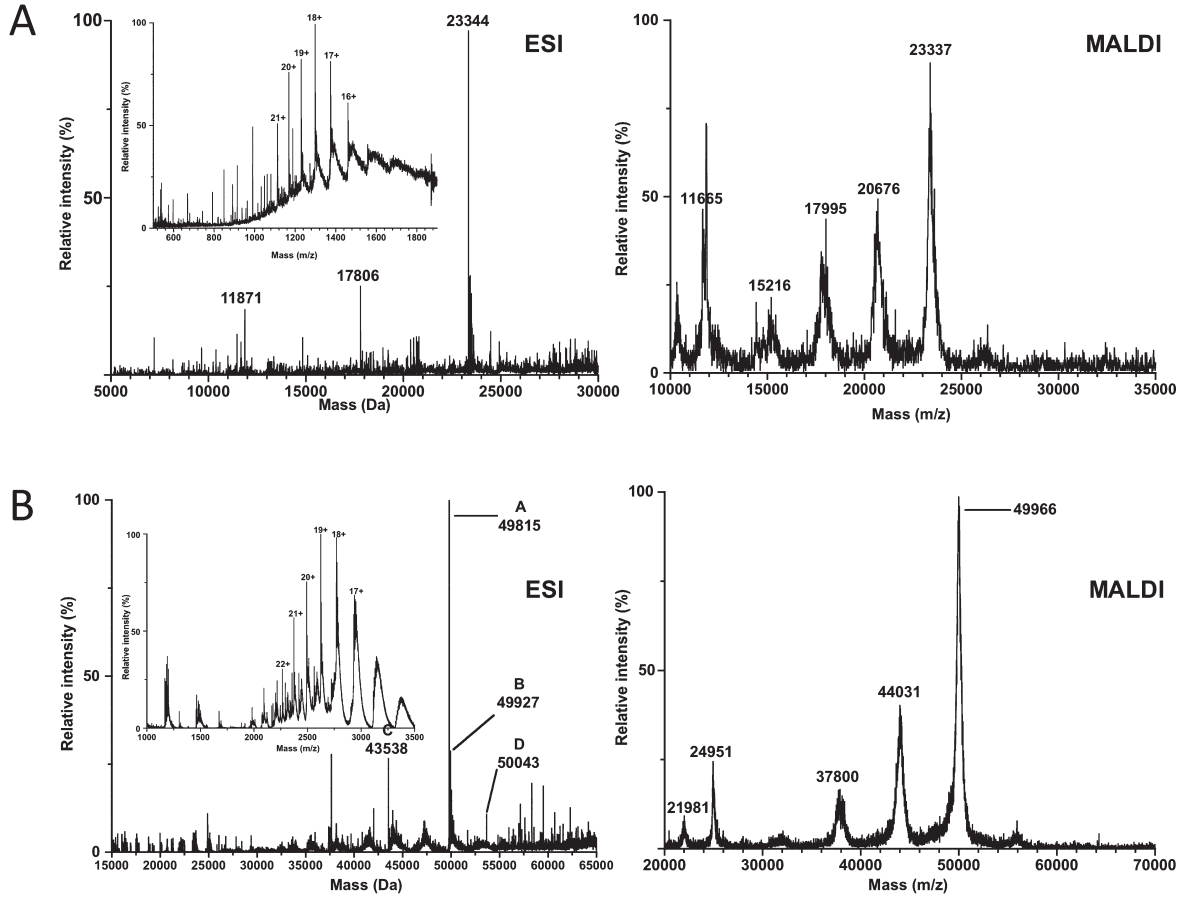

Figure 2. Experimental (inset) and deconvoluted ESI-TOF-MS of G-1(AEEA-Pyr=AoA-MVHA49−72)$_8$ (A) and G-1(AEEA-Pyr=AoA-Insulin)$_8$ (B) as compared with MALDI-TOF-MS. While ESI-TOF-MS analysis indicates that the samples predominantly contain fully decorated dendrimer with no traces of lower substituted contaminants, MALDI-TOF-MS analysis of the same samples reveals a mass component corresponding to the fully substituted dendrimer, plus mass components corresponding to the dendrimer lacking one, two, and three substituent moieties.

dendrimers resulting from the decoration of G-1(Pyr)$_8$ dendrimers with either AoA-MVHA49−72, yielding G-1(Pyr=AoA-MVHA49−72)$_8$, or AoA-insulin, yielding G-1(AEEA-Pyr=AoA-Insulin)$_8$. ESI-TOF-MS (Figure 2A) clearly indicated that in both cases the major component in the reaction mixture was indeed the fully decorated octamer (for AoA-MVHA49−72 observed average mass 23 343.8 ± 0.7 Da, calculated mass 23 344.5 Da; for AoA-insulin observed average mass 49 809 ± 5 Da, calculated mass 49 821.2 Da). The absence in the mixture of detectable levels of incompletely decorated material is indicative of the homogeneity of the reaction products. Analysis of the same material by MALDI-TOF-MS (Figure 2B) revealed peaks corresponding to the expected masses of the fully decorated octamers (observed average mass 23 401 Da for AoA-MVHA49−72; observed mass 48 862 Da for AoA insulin) plus a series of peaks corresponding to the expected masses minus multiples of the mass of the substituent moiety (i.e., approximately 2700 Da for MHVA(49−71) and 5800 Da for insulin). The absence of these lower mass species in the ESI-TOF mass spectra indicates that they do not correspond to incompletely decorated dendrimers but artifacts resulting from the destructive effect on the oxime bonds of the MALDI laser pulses, as described previously.[25] Hence, while ESI-TOF-MS has the advantage of being a non-destructive characterization method for the dendrimers in this study, it has the drawback of having, at least in our case, a ceiling size limit for detection at around 50 kDa. On the other hand, while MALDI-TOF-MS has the advantage of being able to detect dendrimers of higher mass, analysis of the results obtained should take account of the destructive effect of the laser pulses on oxime bonds.

Synthesis of Peptide and Protein-Conjugated Dendrimers. We next used the optimized oxime conjugation conditions to decorate a wider range of dendrimers (up to G-3), with or without arms extended by short PEG spacers, using the short LYRAG peptide, the longer measles virus hemeagluttenin (49−72) peptide, and recombinant insulin. The reaction products were characterized by mass spectrometry (Table 2).

These results indicate that the optimized oxime procedure yields fully decorated dendrimers from G-1 to G-3 either with or without PEG-extended arms and using three different aminooxy conjugated substituents. While the MALDI-TOF-MS spectra included signals corresponding to lower-substituted products, these would be expected to be due at least in part to the destructive effect of the laser desorption on oxime bonds (Figure 2).

Size exclusion chromatography of the reaction products revealed single symmetrical peaks for each product, with rank order of elution time (fastest to slowest) corresponding to rank order target size (largest to smallest; see Supporting Information, Figure S2).

Characterization of Insulin Dendrimers by SDS-PAGE. In order to further investigate the homogeneity of the dendrimer

Table 2. Peptide and Insulin Dendrimers Obtained by Aniline Catalyzed Oxime Bond Formation[a]

dendrimer	calculated average mass (Da)	observed average mass (Da) ESI-MS, ESI-TOF-MS MSMS	observed average mass (Da) MALDI-TOF-MS
G-1(Pyr=AoA-LYRAG)$_8$	7060.2	7060.1 ± 0.3	7061
G-2(Pyr=AoA-LYRAG)$_{16}$	14516.6	14517.4 ± 1.1	14520
G-3(Pyr=AoA-LYRAG)$_{32}$	29430.3	nd	envelope of 16000−29500
G-1(AEEA-Pyr=AoA-LYRAG)$_8$	8221.6	8221.5 ± 0.6	nd
G-2(ATOPA-Pyr=AoA-LYRAG)$_{16}$	18473.6	18472.6 ± 0.8	nd
G-1(Pyr=AoA-MVHA49−72)$_8$	23344.5	23344.4 ± 0.7	23450 ± 250
G-2(Pyr=AoA-MVHA49−72)$_{16}$	47113.3	nd	47200 ± 2003
G-3(Pyr=AoA- MVHA49−72)$_{32}$	94594.7	nd	envelope of 56000−95000
G-1(AEEA-Pyr=AoA-Insulin)$_8$	49821.2	49815.0 ± 1.0	49970 ± 500
G-2(ATOPA-Pyr=AoA-Insulin)$_{16}$	101672.8	nd	101500 ± 1000
G-1(Pyr=AoA-Insulin)$_8$	48659.8	nd	48700 ± 100
G-2(Pyr=AoA-Insulin)$_{16}$	97743.8	nd	98000 ± 1000
G-3(Pyr=AoA-Insulin)$_{32}$	195855.8	nd	envelope of 130000−190000

[a] All MALDI-TOF-MS mass determinations contain signals (probably artifactual, see text) attributable to lower substituted constructs (nd; not determined).

products, we used SDS-PAGE to analyze a series of insulin-decorated dendrimers of increasing complexity: G-1 (Pyr=AoA-Insulin)$_8$, G-1 (Pyr=AoA-Insulin)$_{16}$, and G-1 (Pyr=AoA-Insulin)$_{32}$ (Figure 3). Each sample appeared on the gel as a slower-migrating major component together with relatively few minor bands. On the basis of the mass spectrometric analysis of the same samples (Table 2), the major components most likely correspond to the fully decorated dendrimers. If this is the case, it would imply that size-dependent migration of the dendrimers on SDS-PAGE is not proportional to that of the globular protein markers, with the fully decorated G-1, G-2, and G-3 dendrimers, which have calculated masses of approximately 49, 98, and 196 kDa, respectively, migrating at positions corresponding to approximately 36, 50, and 100 kDa.

Comparison of the appearance of the G-1 (Pyr=AoA-Insulin)$_8$ sample on the gel with the corresponding ESI-TOF mass spectrum (Figure 2) indicates that sample treatment prior to gel loading is partially destructive. This is mostly likely because heating the samples in gel loading buffer led to brief exposure to basic pH levels at which oxime bonds are labile.[7] Despite this, the tight clustering bands close to the slowest migrating species, together with the absence of bands corresponding to unsubstituted material, provide further evidence of the high homogeneity of the decorated dendrimer samples.

Diblock Approach. The option of independently attaching multiple functional units to dendrimers via precision conjugation would be of significant value in the development of bioactive nanoparticles, and several different strategies have been employed to generate asymmetric bifunctional dendrimers.[8,13,14] With this aim in mind, we next worked on the development of a generic diblock heterodendrimer approach to be used as a scaffold for the display of an oxime-linked protein or peptide array together with an array corresponding to a second functional unit (Scheme 1).

A sample of G-3 PAMAM dendrimer with a cystamine core was divided into two batches, with one batch acylated with ATOPA and the other Boc-protected (**I** and **II** in Scheme 1). The modified dendrimer batches were then reduced, opening the cystamine core to yield sulfhydryl-bearing half-dendrimers. The ATOPA half-dendrimer (**I** in Scheme 1) was then alkylated with a moderate excess of bismaleimido-PEG linker, and the resulting monomaleidimido product (**III** in Scheme 1) was used to alkylate the Boc-protected half dendrimer (**II** in Scheme 1). This yields the heterodendrimer precursor, G-3(ATOPA-NH$_2$)$_{16}$-S-PEG-S-G-3(Boc)$_{16}$ (**IV** in Scheme 1).

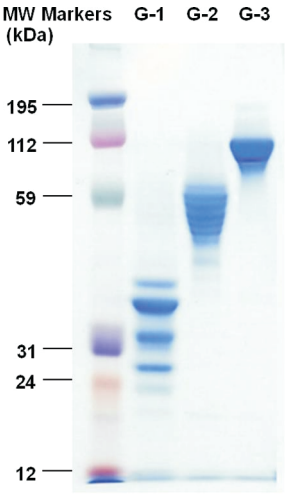

Figure 3. SDS-PAGE analysis of G-1 (Pyr=AoA-Insulin)$_8$, G-2 (Pyr=AoA-Insulin)$_{16}$, and G-1 (Pyr=AoA-Insulin)$_{32}$ (indicated as G-1, G-2, and G-3) indicating that dendrimer samples from each reaction show very limited dispersity.

This heterodendrimer precursor provides a versatile diblock platform for producing nanoparticles carrying two different sets of functional units. The first type of functional unit can be attached by acylation of the ATOPA amine groups on one-half of the heterodendrimer; then, a deprotection step can be used to reveal the amine groups on the other half of the heterodendrimer for attachment of the second type of functional unit.

Mannosylated Dendrimers. We chose to use the diblock approach to produce a heterodendrimer carrying a peptide on one side and a mannose array on the other (Scheme 2). Nanoparticles of this kind are of interest in the development of vaccine delivery vehicles, where the peptide or protein cargo would be an immunizing antigen and purpose of the mannose array is to

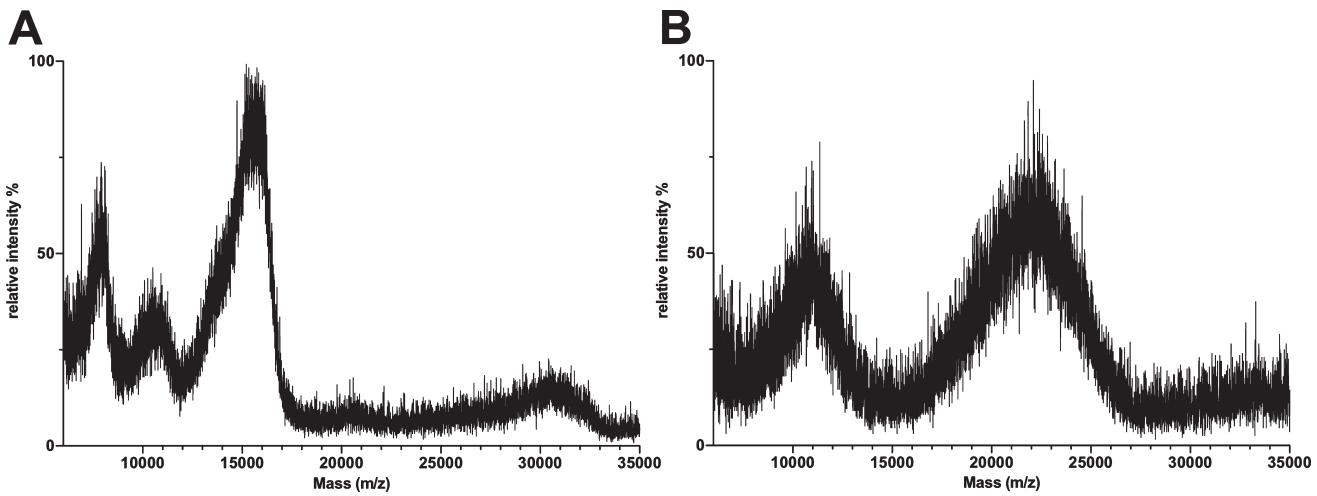

Figure 4. MALDI-TOF-MS characterization of G-3 (ATOPA-Mannose)$_{16}$-S-PEG-S-G-3(Pyruvate)$_{16}$ and the peptide-conjugated product. Respective theoretical average masses of fully substituted compounds are 16 633 and 26 772 Da.

specifically target the particle to macrophages and dendritic cells, whose efficient uptake of particulate antigens is crucial in the generation of strong immune responses.[19,20] While dendrimer conjugation with mannose has been achieved using both 4-isothiocyanatophenyl-α-D-mannopyranoside and 3-(2,3,4,6-tetra-*O*-acetyl-α-D-mannopyranosylthio)propionic acid,[5] the phenyl ring in the thiourea linker of the former reagent leads to a significantly hydrophobic product, and in the interest of hydrosolubility of the final product, we opted for the latter. The resulting mannosylated heterodendrimer (**V** in Scheme 2) was then Boc-deprotected and acylated with pyruvate, yielding a mannosylated pyruvate dendrimer (**VI** in Scheme 2) ready for oxime conjugation with aminooxy-peptides or proteins. For the purposes of this study, we used the model peptide AoA-LYRAG to produce the final product, a mannose−peptide heterodendrimer (**VII** in Scheme 2).

As expected, the heavily glycosylated mannose heterodendrimers migrated as diffuse bands on SDS-PAGE (data not shown), and as a consequence, this analytical method was not useful for their characterization. With regard to mass spectrometric analysis, while the starting heterodendrimer G-3 (ATOPA-NH_2)$_{16}$-S-PEG-S-G-3(Boc)$_{16}$ had a mass low enough to be characterized by ESI-MS (observed average mass 13 112.9 Da; calculated mass 13 108.9 Da), ESI-MS could not be used for analysis of the higher-molecular-weight glycodendrimers due to limitations of the technology, as noted previously.[26] According to MALDI-TOF-MS, mannose functionalization resulted in increased dispersity seen as a broadened peak with an envelope ranging between 6600 and 11 800 Da, apex at 9800 Da, for an expected value of 11 852 Da (Figure 4). The level of polydispersity introduced into our constructs at this stage is comparable with that seen in the work of others on carbohydrate conjugation of dendrimers,[6,26] including experiments in which dendrimers were directly modified with unprotected *p*-isothiocyanatophenyl α-D-mannopyranoside.[5]

As expected, conjugating the mannosylated pyruvate heterodendrimer with AoA-LYRAG generated a mass shift (Figure 4), but while the theoretical shift is from 16 633 to 26 772 Da, the apexes of the observed peaks shifted from 15 500 to 22 100 Da, with the envelope of the product peak broadening further to span the range 16 000−26 000 Da. The lower apex mass value and further broadening of the product peak are most likely consequences of damage to oxime linkages during the MALDI process, as seen earlier with the insulin octamers (Figure 2). Hence, our results are consistent with complete peptide decoration of the mannosylated heterodendrimer.

Polymannose-Decorated Dendrimers Efficiently and Specifically Target Dendritic Cells and Macrophages. In order to investigate whether addition of a mannose array to dendrimers enhances uptake by sentinel cells, it was necessary to site-specifically incorporate a fluorescent label. We designed a panel of fluorescein-labeled constructs, three half-dendrimers labeled by alkylation of their core sulfhydryl group, and two diblock constructs labeled on the linker used to join the two half-dendrimers together (a G-3(ATOPA-NH_2)$_{16}$-S-PEG-S-G-3(Boc)$_{16}$ heterodendrimer in which N^{ε}-fluoresceinyl-lysine was introduced into the structure of the linker) (Scheme 3).

We had initially attempted to produce the labeled heterodendrimers by replacing the bismaleimidoPEG linker (see Scheme 2) with a maleimido-AEEA-Lys(FAM)-ADOOA-maleimide linker, but as previously seen for immunoconjugates,[27] these maleimide-linked structures showed limited stability at basic pH. Since mild basic conditions are required for the per-O-acetylmannose deprotection, we opted to make use of a diiodoacetyl analogue of the linker (see Supporting Information for further details) instead. Analysis by MALDI-TOF-MS confirmed that the fluorescent heterodendrimers made in this way were decorated with mannose and peptide to levels comparable with the nonfluorescent versions (see Supporting Information).

These fluorescent constructs (II through V in Scheme 3) were evaluated for specific *in vitro* uptake by sentinel cells using a flow cytometry technique on cell populations prepared from mouse lymph nodes (Figure 5). Lymphocytes predominate in this mixed population, which also contains dendritic cells and macrophages. While fluorescence uptake across the whole cell population was relatively low (Figure 5A), it was strongly and specifically enriched in the dendritic cell and macrophage groups (Figure 5B, C). Within these groups, mannose-functionalized half-dendrimers show a strongly increased uptake compared with the corresponding pyruvate functionalized dendrimers (Figure 5B,C). In the same way, uptake of the pyruvate-functionalized mannosylated heterodendrimer is strongly increased compared to the corresponding pyruvate-conjugated half-dendrimer. Importantly,

Scheme 3. Fluorescent Dendrimers Used in the Study of Mannose-Specific Uptake by Sentinel Cells[a]

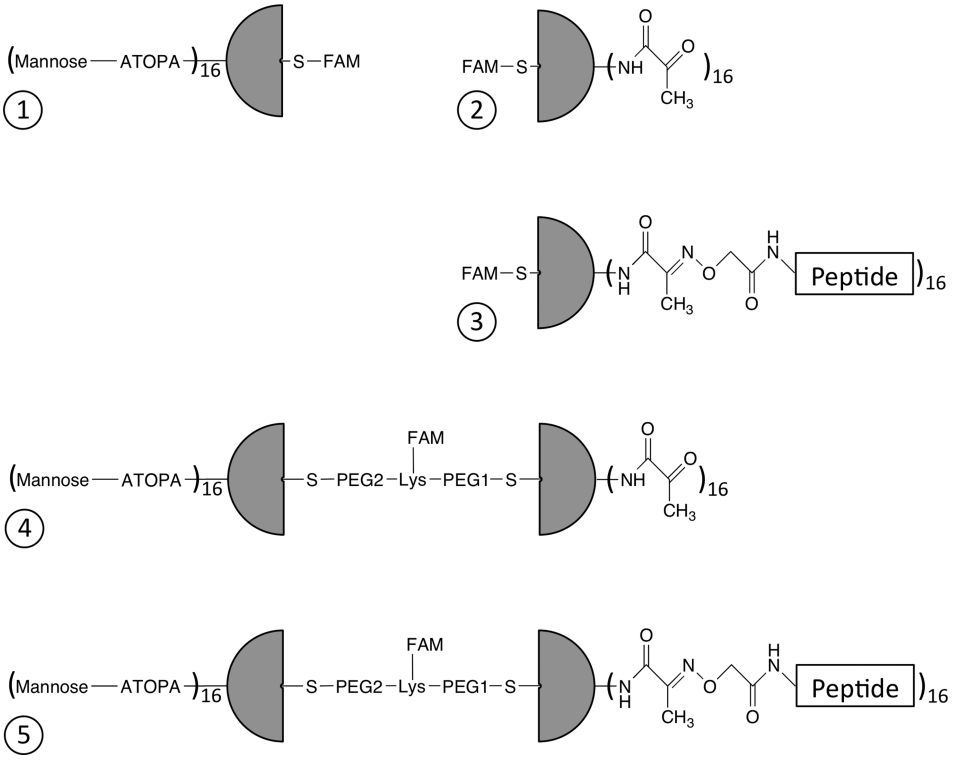

[a] (1) Mannose G-3 half-dendrimer; (2) pyruvate G-3 half-dendrimer; (3) LYRAG peptide G-3 half-dendrimer; (4) mannose-pyruvate G-3 heterodendrimer; (5) mannose-LYRAG peptide G-3 heterodendrimer. Details of the structure and synthesis of the fluorescein linker (FAM) are provided in Supporting Information.

incorporation of mannose into dendrimers did not increase fluorescence incorporation into lymphocytes, which do not express mannose receptors (Figure 5D). Uptake of mannosylated dendrimer was blocked when incubation carried out at 4 °C (data not shown) and in the presence of mannan, a mannose receptor ligand (data not shown) suggesting an active uptake process by the macrophage and dendrimer cells groups mediated by mannose receptors.

Hence, in agreement with previous observations,[18,21] our results indicate that incorporation of a mannose array into nanoparticles strongly and specifically enhances uptake by macrophages and dendritic cells, most likely via surface lectin-mediated endocytosis. Enhanced uptake is not hindered by incorporation of a second half-dendrimer displaying a peptide array. Conjugating the pyruvate dendrimers with the LYRAG peptide also leads to a modest increase in incorporation, whether or not the particles carry mannose. The effect is nonspecific, i.e., nonsentinel cells showed similar levels of uptake as sentinel cells. LYRAG is a basic sequence, and this phenomenon is almost certainly a consequence of the polycation-mediated cell uptake a well-known and generalized phenomenon, exploited in gene delivery[28] and peptide transduction[29] strategies.

■ DISCUSSION

Dendrimers are readily synthesized, low-cost, monodisperse, high-valency molecular scaffolds, and as such represent promising building blocks for the generation of bioactive nanoparticles for use as both clinical and experimental tools.[1,2] However, a major obstacle in their use in these applications has been the absence of a conjugation chemistry powerful enough to fully decorate high-valency dendrimers with protein and peptide ligands.

In this study, we have made use of recent advances in oxime technology to develop an optimized conjugation strategy for decorating PAMAM dendrimers with peptides and proteins. The size range of the target products is close to or beyond the upper limit for the characterization methods typically used in protein chemistry, and although we opted to use different characterization methods, each one was subject to particular limitations: (i) the ESI-TOF-MS facilities that we used had an upper detection limit of 50 kDa for dendrimer-derived products; (ii) the MALDI-TOF-MS desorption process is partially destructive toward molecules containing oxime bonds [25] (Figure 2), as is (iii) heating samples in loading buffer prior to SDS-PAGE (Figure 3). Nonetheless, the combined evidence obtained from these three methods indicates that our conjugation strategy readily yielded highly homogeneous preparations of fully decorated dendrimers of up to 32 valency (G-3) obtained using both a synthetic 23mer virus-derived peptide and porcine insulin. This is an important breakthrough, since previous work on dendrimer conjugation has not yielded fully decorated dendrimers more complex than octamers. Because of the difficulties involved in the characterization of very large molecular products, we did not attempt to conjugate dendrimers of higher generation than G-3 in this study. Full decoration of larger, higher valency scaffolds should nonetheless be feasible, as long as the surface density of reactive groups does not reach a level where conjugation is limited by steric blockade. Should that occur, the problem could readily be addressed by

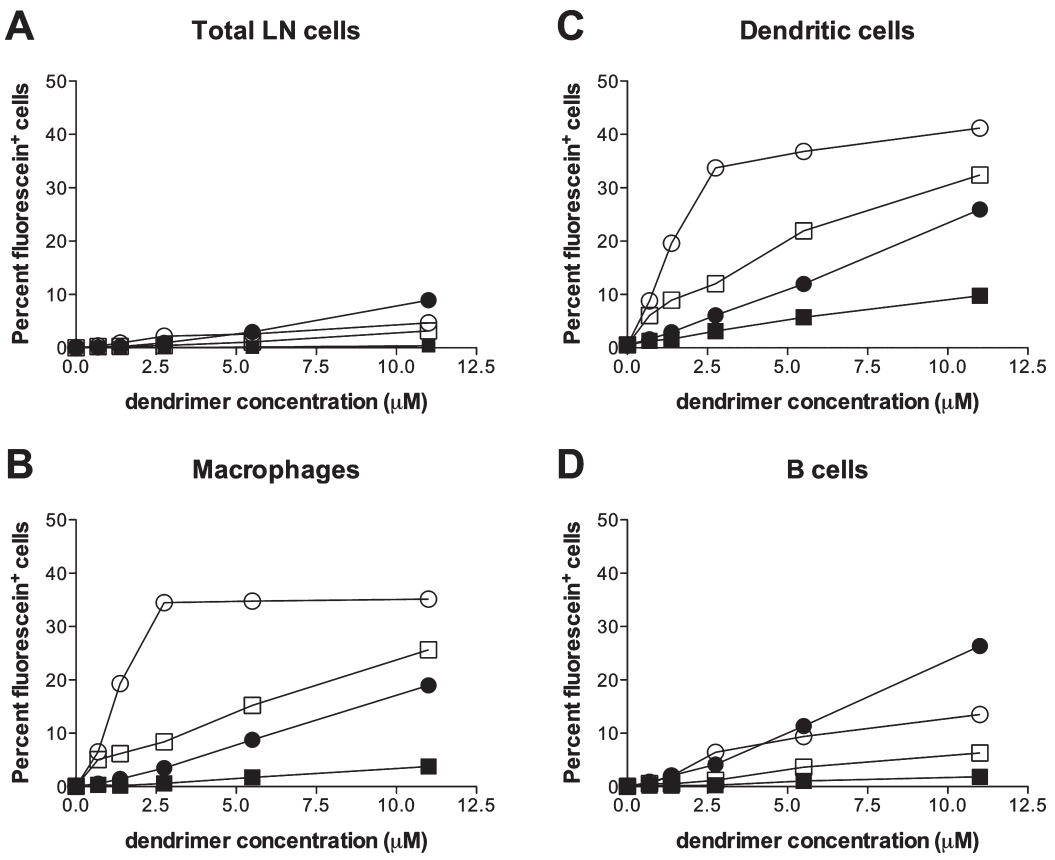

Figure 5. Specific mannose-dependent uptake of dendrimer nanoparticles by sentinel cells. Uptake of fluorescein-conjugated dendrimers (see Scheme 3) by cells prepared from mouse lymph nodes was detected by flow cytometry (FL-1 channel) on gated subpopulations (as indicated) after incubating the total cell population with dendrimers at different concentrations for 1 h at 37 °C. Filled squares, pyruvate G-3 half-dendrimer (16mer) (**2**); filled circles, LYRAG peptide G-3 half-dendrimer (16mer) (**3**); empty squares, mannose-pyruvate G-3 heterodendrimer (16mer + 16mer) (**4**); empty circles, mannose-LYRAG G-3 heterodendrimer (16mer + 16mer) (**5**).

elongation of the dendrimer arms through the attachment of flexible precision PEG chains such as AEEA or ATOPA (Table 2).

Importantly, the oxime conjugation strategy that we have developed is likely to be robust enough to be readily usable with a wide range of peptides and proteins, of both synthetic and recombinant origin. Use of recombinant proteins will generally require the introduction of an appropriate molecular hook for aminooxy modification. This could involve engineering either an extra surface cysteine residue to provide a free sulfhydryl group or an N-terminal serine or threonine residue, which could be quantitatively oxidized under extremely mild conditions to yield an aldehyde[30] for further functionalization.

Diblock Dendrimers: A Platform for Orthogonal Attachment of Two Functional Sets. Techniques that enable the specific incorporation of more than one functional unit (e.g., targeting ligand, payload, tracer) into the dendrimer architecture would be advantageous in the development of bioactive nanoparticles,[1,2] and a number of strategies for the generation of heterodendrimers have been proposed.[8,13,14] These approaches have the drawback of not being compatible with the use of commercially available starting materials, and in this context, it is significant that the orthogonal diblock strategy developed in this study centers on readily produced, commercially available cystamine core PAMAM dendrimers.

We chose to use mannose as the first functional unit, as there has been considerable interest in the development of carbohydrate-conjugated dendrimers,[5,6] and incorporation of a mannose array into a nanoparticle-based vaccine vehicle has the potential to increase immunogenicity by enhancing uptake processing and presentation by sentinel cells such as macrophages and dendritic cells.[19−21] An array of short synthetic peptide molecules attached via oxime conjugation was used as the second functional unit. Notwithstanding the additional challenge to characterization imposed by the incorporation of mannose residues into the dendrimers, we were able to confirm (Figure 4) that (i) the mannose-conjugated heterodendrimers could be fully decorated with a peptide array using the optimized oximation approach and (ii) mannose conjugation levels comparable to those reported in previous studies were obtainable. More efficient mannose conjugation might be achieved through the use of Cu(I) catalyzed azide−alkyne cycloaddition[10] because it is compatible with direct use of unprotected carbohydrate.

In order to visualize uptake of these particles by sentinel cells, it was necessary to devise a conjugation approach for site-specific conjugation of a third functional unit so that the particles could be derivatized with a fluorochrome. With the resulting trifunctionalized dendrimers, we were able to demonstrate that, in agreement with previously published work,[18−21] incorporation of a mannose array strongly and specifically enhances uptake of the dendrimers by sentinel cells. Mannose heterodendrimers may represent promising vaccine delivery vehicles for peptide and protein cargoes, and the conjugated linker could be used either to attach a fluorescent dye to aid the study of vehicle uptake *in vivo*[31]

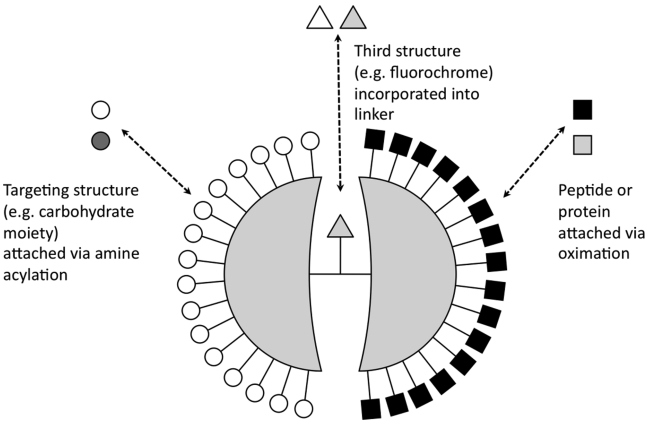

Figure 6. Versatile platform for synthesis of bioactive nanoparticles.

or to attach an immune modulator structure (e.g., a Toll-like receptor ligand) to enhance adjuvant activity.[32]

CONCLUSION

We believe that we have developed a robust new dendrimer conjugation strategy which can be used not only for the production of large multivalent dendrimers fully decorated with proteins and peptides, but also for the generation of specifically bi- and trifunctionalized dendrimers (Figure 6).

Given the mild conjugation conditions involved, the strategy should be applicable for dendrimer derivatization using a wide range of biologically relevant structures, providing a convenient platform for the production of bioactive nanoparticles for use in a wide range of clinical applications.

ASSOCIATED CONTENT

Supporting Information. Characterization of pyruvate-functionalized PAMAM dendrimers; size exclusion chromatography analysis of peptide-decorated dendrimers; synthesis of PEG linkers for dendrimer arm extension; synthesis and characterization of bifunctional linkers; synthesis and characterization of linker-conjugated mannose; mass spectrometry characterization of key intermediates IV (Scheme 1 in main text) and V (Scheme 2 in main text); characterization of fluorescein-labeled homo- and heterodendrimers. This material is available free of charge via the Internet at http://pubs.acs.org.

AUTHOR INFORMATION

Corresponding Author

*E-mail: oliver.hartley@unige.ch. Tel: +41 22 379 54 75. Fax +41 22 379 55 02.

ACKNOWLEDGMENT

We thank Robin Offord and Sylvie Tchertchian for critical discussion and the NMR group of Dr. Damien Jeannnerat at the University of Geneva for providing NMR spectra. We gratefully acknowledge support from Dormeur Investment Service Ltd.

REFERENCES

(1) Lee, C. C., MacKay, J. A., Frechet, J. M., and Szoka, F. C. (2005) Designing dendrimers for biological applications. *Nat. Biotechnol. 23*, 1517–26.

(2) Boas, U., and Heegaard, P. M. (2004) Dendrimers in drug research. *Chem. Soc. Rev. 33*, 43–63.

(3) Esfand, R., and Tomalia, D. A. (2001) Poly(amidoamine) (PAMAM) dendrimers: from biomimicry to drug delivery and biomedical applications. *Drug Discovery Today 6*, 427–436.

(4) Mammen, M., Choi, S.-K., and Whitesides, G. M. (1998) Polyvalent interactions in biological systems: implications for design and use of multivalent ligands and inhibitors. *Angew. Chem., Int. Ed. 37*, 2754–2794.

(5) Woller, E. K., and Cloninger, M. J. (2001) Mannose functionalization of a sixth generation dendrimer. *Biomacromolecules 2*, 1052–4.

(6) Woller, E. K., Walter, E. D., Morgan, J. R., Singel, D. J., and Cloninger, M. J. (2003) Altering the strength of lectin binding interactions and controlling the amount of lectin clustering using mannose/hydroxyl-functionalized dendrimers. *J. Am. Chem. Soc. 125*, 8820–6.

(7) Rose, K., Zeng, W., Regamey, P. O., Chernushevich, I. V., Standing, K. G., and Gaertner, H. F. (1996) Natural peptides as building blocks for the synthesis of large protein- like molecules with hydrazone and oxime linkages. *Bioconjugate Chem. 7*, 552–6.

(8) Mitchell, J. P., Roberts, K. D., Langley, J., Koentgen, F., and Lambert, J. N. (1999) A direct method for the formation of peptide and carbohydrate dendrimers. *Bioorg. Med. Chem. Lett. 9*, 2785–8.

(9) van Baal, I., Malda, H., Synowsky, S. A., van Dongen, J. L., Hackeng, T. M., Merkx, M., and Meijer, E. W. (2005) Multivalent peptide and protein dendrimers using native chemical ligation. *Angew. Chem., Int. Ed. Engl. 44*, 5052–7.

(10) Chun, C. K. Y., and Payne, R. J. (2009) Synthesis of MUC1 peptide and glycopeptide dendrimers. *Aust. J. Chem. 62*, 1339–1343.

(11) Yim, C. B., Boerman, O. C., de Visser, M., de Jong, M., Dechesne, A. C., Rijkers, D. T., and Liskamp, R. M. (2009) Versatile conjugation of octreotide to dendrimers by cycloaddition ("click") chemistry to yield high-affinity multivalent cyclic peptide dendrimers. *Bioconjugate Chem. 20*, 1323–31.

(12) Lempens, E. H., van Baal, I., van Dongen, J. L., Hackeng, T. M., Merkx, M., and Meijer, E. W. (2009) Noncovalent synthesis of protein dendrimers. *Chemistry 15*, 8760–7.

(13) Wu, P., Malkoch, M., Hunt, J. N., Vestberg, R., Kaltgrad, E., Finn, M. G., Fokin, V. V., Sharpless, K. B., and Hawker, C. J. (2005) Multivalent, bifunctional dendrimers prepared by click chemistry. *Chem. Commun. (Camb.)* 5775–7.

(14) Dirksen, A., Meijer, E. W., Adriaens, W., and Hackeng, T. M. (2006) Strategy for the synthesis of multivalent peptide-based nonsymmetric dendrimers by native chemical ligation. *Chem. Commun. (Camb.)* 1667–9.

(15) Kochendoerfer, G. G., Tack, J. M., and Cressman, S. (2002) Total chemical synthesis of a 27 kDa TASP protein derived from the MscL ion channel of M. tuberculosis by ketoxime-forming ligation. *Bioconjugate Chem. 13*, 474–80.

(16) Dirksen, A., Dirksen, S., Hackeng, T. M., and Dawson, P. E. (2006) Nucleophilic catalysis of hydrazone formation and transimination: implications for dynamic covalent chemistry. *J. Am. Chem. Soc. 128*, 15602–3.

(17) Dirksen, A., Hackeng, T. M., and Dawson, P. E. (2006) Nucleophilic catalysis of oxime ligation. *Angew. Chem., Int. Ed. Engl. 45*, 7581–4.

(18) Angyalosi, G., Grandjean, C., Lamirand, M., Auriault, C., Gras-Masse, H., and Melnyk, O. (2002) Synthesis and mannose receptor-mediated uptake of clustered glycomimetics by human dendritic cells: effect of charge. *Bioorg. Med. Chem. Lett. 12*, 2723–7.

(19) Geijtenbeek, T. B. H., and Gringhuis, S. I. (2009) Signalling through C-type lectin receptors: shaping immune responses. *Nat. Rev. Immunol. 9*, 465–479.

(20) Rieger, J., Freichels, H., Imberty, A., Putaux, J.-L., Delair, T., Jérôme, C., and Auzély-Velty, R. (2009) Polyester nanoparticles presenting

mannose residues: toward the development of new vaccine delivery systems combining biodegradability and targeting properties. *Biomacromolecules 10*, 651–657.

(21) Sheng, K. C., Kalkanidis, M., Pouniotis, D. S., Esparon, S., Tang, C. K., Apostolopoulos, V., and Pietersz, G. A. (2008) Delivery of antigen using a novel mannosylated dendrimer potentiates immunogenicity in vitro and in vivo. *Eur. J. Immunol. 38*, 424–36.

(22) Kaiser, E., Colescott, R. L., Bossinger, C. D., and Cook, P. I. (1970) Color test for detection of free terminal amino groups in the solid-phase synthesis of peptides. *Anal. Biochem. 34*, 595–598.

(23) Gaertner, H., Offord, R., Botti, P., Kuenzi, G., and Hartley, O. (2008) Semisynthetic analogues of PSC-RANTES, a potent anti-HIV protein. *Bioconjugate Chem. 19*, 480–9.

(24) Kamath, A. T., Valenti, M. P., Rochat, A. F., Agger, E. M., Lingnau, K., von Gabain, A., Andersen, P., Lambert, P. H., and Siegrist, C. A. (2008) Protective anti-mycobacterial T cell responses through exquisite in vivo activation of vaccine-targeted dendritic cells. *Eur. J. Immunol. 38*, 1247–56.

(25) Nardin, E. H., Calvo-Calle, J. M., Oliveira, G. A., Clavijo, P., Nussenzweig, R., Simon, R., Zeng, W., and Rose, K. (1998) Plasmodium falciparum polyoximes: highly immunogenic synthetic vaccines constructed by chemoselective ligation of repeat B-cell epitopes and a universal T-cell epitope of CS protein. *Vaccine 16*, 590–600.

(26) Ashton, P. R., Boyd, S. E., Brown, C. L., Nepogodiev, S. A., Meijer, E. W., Peerlings, H. W. I., and Stoddart, J. F. (1997) Synthesis of glycodendrimers by modification of poly(propylene imine) dendrimers. *Chem.—Eur. J. 3*, 974–984.

(27) Presentini, R., and Terrana, B. (1995) Influence of the antibody-peroxidase coupling methods on the conjugate stability and on the methodologies for the preservation of the activity in time. *J. Immunoassay 16*, 309–24.

(28) Pack, D. W., Hoffman, A. S., Pun, S., and Stayton, P. S. (2005) Design and development of polymers for gene delivery. *Nat. Rev. Drug Discovery 4*, 581–593.

(29) Wadia, J. S., and Dowdy, S. F. (2002) Protein transduction technology. *Curr. Opin. Biotechnol. 13*, 52–56.

(30) Gaertner, H. F., and Offord, R. E. (1996) Site-specific attachment of functionalized poly(ethylene glycol) to the amino terminus of proteins. *Bioconjugate Chem. 7*, 38–44.

(31) Misumi, S., Masuyama, M., Takamune, N., Nakayama, D., Mitsumata, R., Matsumoto, H., Urata, N., Takahashi, Y., Muneoka, A., Sukamoto, T., Fukuzaki, K., and Shoji, S. (2009) Targeted delivery of immunogen to primate M cells with tetragalloyl lysine dendrimer. *J. Immunol. 182*, 6061–6070.

(32) Pashine, A., Valiante, N. M., and Ulmer, J. B. (2005) Targeting the innate immune response with improved vaccine adjuvants. *Nat. Med. 11*, S63–8.